MAUSAM, 48, 2 (April 1997), 195-204

551.515.2 : 551.509.327

A numerical typhoon track prediction model and its application on the real-time operation

SHIWEN WANG, DEHUI CHENG, JIANJUN LI and SHUHONG MA

National Meteorological Center, China Meteorological Administration, Beijing 100081, China

सार — हाल ही में राष्ट्रीय मौसम विज्ञान केन्द्र (एन. एम. सी. बीजिंग) द्वारा उच्चतर क्षैतिज विभेदन और सम्मिश्र भौतिक पैकेज वाला, टाइफून के मार्ग के पूर्वानुमान के लिए, एक नीडित गणितीय निदर्श (एम.टी.टी.पी.) तैयार किया गया है। इसकी आरम्भिक अवस्था में विकास के लिए एक संशोधित टाइफून बोगस योजना (इवासाकी 1987) का भी अनुप्रयोग किया गया है।

एम. टी. टी. पी. के डिजाइन का निर्धारण 1992 के अंत में किया गया था और इस निदर्श की पूर्वानुमान क्षमता का 1993 के (बांग और ली 1994) चुने हुए टाइफून मामलों के संबंध में लगातार प्रयोगों के उपरांत पहली बार परीक्षण किया गया है। इसके उपरांत अगले वर्ष वास्तविक काल पूर्वानुमान में इसकी जाँच की गई। 1995 में कुछ और सुधार किए गए, जिसमें उच्चतर क्षैतिज विभेदन का लगभग 50 कि.मी. से 100 कि.मी. तक विस्तार किया जाना, साधारण पैकेज के स्थान पर सम्मिश्र भौतिक पैकेज लगाया जाना तथा विश्लेषित भ्रमिल के निष्कासन के लिए एक योजना भी शामिल है। पूर्वानुमान क्षमता में सुधार के साथ 1 जून 1995 से एम. टी. टी. पी. कल्प-प्रचलन अवस्था में कार्य कर रहा है । गत दो वर्षों के दौरान इसके उत्पादों का पूर्वानुमान कर्ताओं ने भी प्रयोग किया तथा परिणाम उत्साहजनक पाए गए हैं।

ABSTRACT. Recently a nested numerical model for typhoon track prediction (MTTP) with a higher horizontal resolution and a complex physical package has been developed by the National Meteorological Center (NMC, Beijing). For its improvement of initialization, a modified typhoon bogus scheme (Iwasaki 1987) also has been applied.

The design of the MTTP had been determined by the end of 1992 and the forecast capability of this model was tested firstly with a series of experiments for the selected typhoon cases in 1993 (Wang and Li 1994). After it was examined in real-time forecast in the next year, further improvements were made in 1995 including a higher horizontal resolution increased from about 100 to 50 km, a package of complex physics instead of the simple one and a scheme for removal of analyzed vortex. With the improved forecast capability, the MTTP run in quasi-operation from the date of 1 June 1995. Its products were also used by the forecasters during the past two years and the results were very encouraging.

Key words — Nested numerical model, Physical processes, Typhoon bogus, Track prediction, Operational application.

1. Introduction

In history, the NWP of the tropical cyclone (TC) has been such a difficult work, because it is sensitive to the meteorological observations over the tropical ocean as well as the model resolution and physical process parameterization. During the past thirty years, because of the significant advances on the computer processing speed and available memory and the continuing research progress in tropical meteorology, especially in the TC knowledge, it is now possible for better TC forecasts with the rapid development of high resolution models with the package of more detailed and advanced physics.

Recent theoretical research (Holland 1984, DeMaria 1985) demonstrated that TC motions were strongly influenced by the two main factors: one was the

asymmetric basic current and the other was the TC horizontal scale and its outer structure. However, due to the scarcity of the conventional observation on the large ocean, the TC circulation was poorly produced by the objective analysis, with its inaccurate location. So the initial condition formed by the regular observational data failed to resolve or simulate the above important factors. This real requirement prompted the development of TC bogus technique.

Based on the above advantage and funds by the project 85-906 of the State Science Committee of China, the (MTTP) has been implemented at NMC from the development of the limited area analysis and forecast system (LAFS) (Guo *et al.* 1992). Especially focusing on the typhoon track prediction, the model is a nested mesh-grid one with a higher horizontal resolution (about 50 km) and a package of complex physics. For the improvement of the model initial condition, a typhoon initialization procedure was made with the recent advanced knowledge on (*i*) removal of the analyzed typhoon vortex and (*ii*) insertion of the bogus TC into original analysis field. The MTTP performed considerable forecasts skillful for typhoon track by using the above schemes.

2. General specification of the MTTP

2.1. *Governing equations*

The governing equations are composed of the momentum, mass and moist continuity, thermodynamic and hydrostatic equations, written in the flux form as follows :

$$\frac{\partial u}{\partial t} - \frac{1}{\cos\theta} Z P_s v \cos\theta + \frac{\partial}{a \cos\theta \, \partial \lambda} (\phi + E) + \frac{RT}{a \cos\theta} \frac{\partial}{\partial \lambda} \ln P_s + \dot{\sigma} \frac{\partial u}{\partial \sigma} = F_u + D_u \quad (1)$$

$$\frac{\partial v}{\partial t} + Z P_s u \frac{\partial}{a \partial \theta} (\phi + E) + \frac{RT}{a} \frac{\partial}{\partial \theta} \ln P_s + \dot{\sigma} \frac{\partial v}{\partial \sigma} = F_v + D_v \quad (2)$$

$$\frac{\partial P_s}{\partial t} + \frac{1}{a \cos\theta} \left\{ \frac{\partial}{\partial \lambda} (P_s u) + \frac{\partial}{\partial \theta} (P_s v \cos\theta) \right\} + \frac{\partial}{\partial \sigma} (P_s \dot{\sigma}) = 0 \quad (3)$$

$$\frac{\partial q}{\partial t} + \frac{1}{P_s} \left\{ \frac{1}{a \cos\theta} \left(P_s u \frac{\partial q}{\partial \lambda} + P_s v \cos\theta \frac{\partial q}{\partial \theta} \right) + P_s \dot{\sigma} \frac{\partial q}{\partial \sigma} \right\} = S + D_q \quad (4)$$

$$\frac{\partial T}{\partial t} + \frac{1}{P_s} \left\{ \frac{1}{a \cos\theta} \left(P_s u \frac{\partial T}{\partial \lambda} + P_s v \cos\theta \frac{\partial T}{\partial \theta} \right) + \frac{\partial T}{\partial \sigma} - \frac{\alpha T \omega}{\sigma} \right\} = Q + D_T \quad (5)$$

$$\frac{\partial \phi}{\partial \ln \sigma} = -RT \quad (6)$$

where, Z is the absolute potential vorticity and E is the unit-mass kinetic energy given in detail below :

$$Z = \frac{1}{P_s} \left\{ f + \frac{1}{a \cos\theta} \left[\frac{\partial v}{\partial u} - \frac{\partial}{\partial} (u \cos\theta) \right] \right\} \quad (7)$$

$$E = \frac{1}{2} \left(u^2 + \frac{1}{\cos\theta} v^2 \cos\theta \right) \quad (8)$$

where, $\alpha = R/C_p$, geostrophic parameter, $f = 2\Omega \cos\theta$ and ω is the vertical velocity in the pressure coordinate defined as,

$$\omega = P_s \dot{\sigma} + \sigma \frac{\partial P_s}{\partial t} + \frac{\sigma}{a \cos\theta} \left\{ P_s u \frac{\partial}{\partial \lambda} \ln P_s + P_s v \cos\theta \frac{\partial}{\partial \theta} \ln P_s \right\} \quad (9)$$

In the above equations, Q includes the diabatic heating arising from radiation and latent heat release, S includes the moisture source/sink arising from cumulus convection and large-scale condensation, F_u and F_v are surface frictional force terms and D_u, D_v, D_q, D_t denote the horizontal diffusion terms. The Eqns. (1)-(9) use the boundary condition as the following :

$$(P_s \dot{\sigma})_{\sigma = 0} = 0, (P_s \dot{\sigma})_{\sigma = 1} = 0 \quad (10)$$

2.2. *Grid point generations*

The sigma coordinate system is utilized in the vertical with 15 irregular levels, defined as

$$\sigma_k = 0.75 \left(\frac{k}{15} \right) + 1.75 \left(\frac{k}{15} \right)^3 - 1.5 \left(\frac{k}{15} \right)^4 \quad (k = 1, 2, 3, \ldots, 15) \quad (11)$$

where, $\sigma = P/P_s$, P is the pressure and the subscript s denotes the surface value. The vertical distribution of variables is that the horizontal wind (U, V), temperature (T) and specific humidity (q) are on the integer levels while the vertical velocity ($\dot{\sigma}$) and geopotential height (ϕ) are on the semi-levels.

The model integrations are performed on the staggered Arakawa C grid using the reapfrod difference for the dynamic and forward difference for the diabatic heating.

2.3. *Lateral boundary*

A one-way boundary scheme is used between the fine mesh and the coarse as well as between the coarse mesh and the global model (T63L16). At the four outest rows of fine-mesh gridpoints, Davies relaxation method is applied to specify the boundary value as

$$S^{\tau+1} = (1-\alpha)\, S_*^{\tau+1} + \alpha\, \tilde{S}^{\tau+1} \tag{12}$$

where $S^{\tau+1}$ is any fine-mesh model available while $S_*^{\tau+1}$ is the original one before this process. $\tilde{S}^{\tau+1}$ is the corresponding value of the coarse-mesh,

$$\tilde{S}^{\tau+1} = S^{\tau} + \Delta \tilde{S} \tag{13}$$

where S^{τ} is any fine-mesh value at τ time and $\Delta\tilde{S}$ is the boundary tendency from the coarse-mesh model. Here α represents the weighting function as follows,

$$\alpha = 1 - \tanh(kk) \tag{14}$$

kk is the specific number of fine-mesh point from the boundary, *kk* = 1, 2, 3, 4.

2.4. *Forecast domain*

The MTTP is a regional multiple nested model. Its first guess fields are supplied by the operational global spectral model system (T63L16) of NMC. The horizontal resolution of the coarse mesh is 0.9375° over the domain 0°N-50.625°N, 84.375°E-161.25°E, while that of the fine mesh is 0.46875° (approximately 50 km) over the domain 10.3125°N-41.25°N, 105°E-150.9375°E. The grid structure, controlling equations, lateral boundary, time integration and physical processes schemes are the same for both the coarse and the fine mesh. The forecast domain could be extended if the condition of computer sources is allowed.

3. Physical processes

In the last three decades, many studies have been done and the significant progress had been attained in the field of physical processes, such as, the work by Kuo (1974), Anthes (1977), Louis (1979), Tibaldi (1982), Tiedtke (1984), Hart *et al.* (1988), Puri *et al.* (1992) and so on. Following their advances, a package of complex physics is implemented in both the coarse-mesh and fine-mesh grid of the model. Here only a brief description will be given.

3.1. *Deep cumulus convection parameterization*

A new version of Kuo (1974) scheme is used for the vertical integration treatment of the local moisture increasement: (*i*) the moisture for the occurrence and development of cumulus convection is supplied by the large-scale environment but not the large-scale moisture convergence; (*ii*) the multiple cumulus layers are allowed to exist simultaneously.

3.2. *Shallow cumulus convection parameterization*

Using the scheme by Tiedtke (1987), the treatment of shallow convection is similar to that of the turbulent diffusion. The effect produced by the shallow convection does not enhance the heating by liquid precipitation, but only adjusts the profile of atmospheric heat and water vapour. The occurrence of shallow convection is specified according to the atmospheric conditional instability. When the layer for shallow convection is determined, it will be used to solve the simultaneous equations with the turbulent flux forms used in the vertical diffusion equation.

3.3. *Vertical turbulent diffusion parameterization*

The treatment of vertical diffusion is similar to that of turbulent transport in the atmospheric boundary layer (K theory). The subgrid-scale processes of vertical diffusion of heat, momentum and moisture are expressed as the forms of diffusion flux so that their parameterization can be specified by determination of the coefficients (K) of diffusion and exchange. The coefficients are calculated with the formulae by Louis (1979), which is relative to the stability. For any variable ϕ vertical diffusion equation using implicit difference scheme can be written as,

$$\left(\frac{\partial \varphi}{\partial t}\right)_v = \frac{1}{\rho}\frac{\partial}{\partial z}\left(\bar{\rho} K_\varphi \frac{\partial \varphi}{\partial z}\right) \tag{15}$$

giving the upper boundary condition for the above formula : when $P = Pt$, the right hand term is set to zero; and the lower boundary condition: when $P = Ps$, the right hand term is set to $C_\varphi \left|\vec{V_1}\right| (\varphi_1 - \varphi_s)$, where the subscripts 1 and s indicate the lowest model level and the surface

respectively. C_φ is the drag coefficient of surface turbulent flux that varies depending on the different value of the Richardson parameter (RI = 0, neutral; RI > 0, stability; RI < 0, instability). K_φ is defined as the turbulent transfer coefficient that is the similarity function of RI and the model layer.

3.4. *Radiation processes*

The schemes of Lacis and Hansen (1974) and Fels and Schwarzko (1975) are introduced here for the radiative transfer calculations of solar wavelengths and terrestrial wavelengths. In order to reduce the CPU time, the tables are used for the calculations of radiation radio. Cloud amounts and heights are fixed zonal averages for each season using climatological data.

3.5. *Surface thermal budget*

The total surface budget can be determined by the terms defined as the following: the surface absorption of solar short-wave and atmospheric longwave radiation (S_g and A_g respectively), the terrestrial surface radiation ($-\sigma_g T_s^4$), the conduction of surface latent heat [$- H_s(T_s)$] and sensible heat [$- H_e(T_s)$] to the atmosphere, the conduction of surface heat to the subsurface soil or ocean [$- \mathrm{Hg}(T_s)$] and the heat transfer specified by the evaporation at the ice surface [$\mathrm{H_{ice}}(T_s)$]. So the heat balance equation at the surface is given by:

$$S_g + A_g - \sigma_g T_s^4 - H_s(T_s) - H_e(T_s) - H_g(T_s) - H_{ice}(T_s) = 0 \qquad (16)$$

where σ_g is the Stefan-Boltzmann constant. An iteration method may be used to solve the equation so as to obtain the surface temperature (T_s) while the influence by the different condition of underlying surface is also considered in the scheme.

3.6. *Soil thermal conductivity*

Three subsurface layers at depths of 0.05, 0.5 and 5 m is used to calculate the subsurface temperature. The conduction equation of soil heat has the form

$$\frac{\partial T_g}{\partial t} = \frac{\partial}{\partial z}\left(K_g \frac{\partial T_g}{\partial z}\right) \qquad (17)$$

where giving the assumption : $K_g(0) = K_g(z), T_g \equiv 280^\circ$. K_g denotes the thermal diffusivity and T_g is the ground temperature. All of the surface coefficients used in the calculation, such as reflectivity, roughness, surface temperature, soil moisture, snow depth and SST etc. are fixed to the monthly climatological data from the global model (T63L16).

3.7. *Large-scale condensation*

The saturated condensation scheme (Guo *et al.* 1992) is applied as the following: when the over-saturation occurs in the air of model, the rainout are made to return the relative humidity to 100%. So the existing of condensed cloud is not permitted in this scheme. Besides that, the process that the liquid water evaporates again during it descends is also considered.

3.8. *Horizontal diffusion parameterization*

A non-linear second order diffusion scheme is used as follows.

$$D_\chi = \kappa \left| \nabla^2 \chi \right| \nabla^2 \chi \qquad (18)$$

where, χ is any variable, κ is the diffusion coefficient and ∇^2 represents Laplace operator as follows :

$$\nabla^2 \chi = \frac{\Delta^2 \chi}{a^2 \cos^2 \theta \Delta\lambda^2} + \frac{\Delta(\cos\theta \Delta\chi)}{a^2 \cos\theta \Delta\theta^2}$$

3.9. *Moisture modification*

Because the advection term at the moisture equation is calculated using the non-regular difference method, the incorrection that the negative moisture occurs can not be avoided. So the modification must be made for those points where moisture are negative. Such a negative value of the central point is compensated to zero by those of the four surrounding points on the vertical meridional cross-section. The contribution from a surrounding point is specified by its value and the average weight determined from its distance to the compensated point. A shorter distance and a larger moisture value may lead to a larger weight coefficient while the opposite occurs, if the contrary situation prevails.

4. Removal of the analyzed typhoon vortex from the objective analysis field

Due to the lack of observation in the ocean, the current analysis has a difficulty in describing the detailed structure of typhoon vortex. The analyzed vortices were evidently too large and weak with their inaccurate central positions and intensities that were different from their corresponsible realistic ones. Such

a initial condition for model would result in the original forecast errors that significantly affect the typhoon motion. So the poorly resolved analyzed vortex should be removed from the large-scale analysis before the bogus typhoon is blended into the analysis field.

The scheme of Kurihara *et al.* (1990, 1993) is introduced for solving the problem. Here, the original analysis field (h) can be split into the large-scale basic field (h_B) and the disturbance field (h_D) as follows,

$$h = h_B + h_D \tag{19}$$

where, h represents any variable. Let the analyzed typhoon vortex (h_{av}) be included in the disturbance (h_D), then the environmental field (h_E) can be obtained by recombining the remaining non-typhoon disturbance and the basic field as :

$$h_E = h_B + (h_D - h_{av}) \tag{20}$$

$$\text{or } h_E = h - h_{av} \tag{21}$$

The filtering is carried out in both the zonal and meridional directions respectively to divide h into h_D and h_B, then h_{av} can be separated from h_D using the cylindrical filtering. In detail, filtering in the zonal direction is firstly applied using a local three-point smoothing operator as follows,

$$\bar{h}_{i,j} = h_{i,j} + k(h_{i-1,j} + h_{i+1,j} - 2h_{i,j}) \tag{22}$$

where, $\bar{h}$ is the zonal-smoothed value and the subscript i and j denote longitude and latitude respectively, k is the filtering coefficient defined by,

$$k = \frac{1}{2}\left(1 - \cos\frac{2\pi}{m}\right)^{-1} \tag{23}$$

where, m sequentially varies as 2, 3, 4, 2, 5, 6, 7, 2, 8, 9, 2 so the components with less than 9 degrees wavelength will be filtered. The above procedure is applied for the filtering in the meridional direction to obtain the basic field as the following.

$$\bar{h}_{Bi,j} = \bar{h}_{i,j} + k\,(\bar{h}_{i,j-1} + \bar{h}_{i,j+1} - 2\,\bar{h}_{i,j}) \tag{24}$$

Then the h_D can be easily obtained from the Eqn. (19).

The isolation of the analyzed typhoon vortex h_{av} from h_D is accomplished through the cylindrical filtering in the polar coordinate system (r, θ) written by,

$$h_{av}(r, \theta) = [1 - E(r)]\,[h_D(r, \theta) - \bar{h}_D(r_0)] \tag{25}$$

where, $E(r)$ is the empirical function to determine the filtering characteristic that h_{av} gradually diminishes to zero at the filter edge as the following:

$$E(r) = \begin{cases} \exp\left\{-(r_0 - r)^2/l^2\right\} - \exp\left\{-(r_0)^2/l^2\right\} & r \le r_0 \\ 1 & r > r_0 \end{cases} \tag{26}$$

In this formula, l controls the filtering shapes and is empirically set to $r_0/5$ here. r_0 is the radius from the center of analyzed typhoon vortex and defines the filtering domain.

The r_0 determination and the center of analyzed typhoon vortex are described below.

Let V_D be the disturbance wind velocity at the 850 hPa level given by,

$$V_D = (u_D^2 + v_D^2)^{1/2} \tag{27}$$

Then the central position (λ_0, φ_0) of the analyzed typhoon vortex can be specified by the distribution of V_D as follows,

$$\lambda_0 = \frac{\sum V_{Di,j}\,\lambda_{i,j}\,\Delta S_{i,j}}{\sum V_{Di,j}\,\Delta S_{i,j}} \tag{28}$$

$$\varphi_0 = \frac{\sum V_{Di,j}\,\varphi_{i,j}\,\Delta S_{i,j}}{\sum V_{Di,j}\,\Delta S_{i,j}} \tag{29}$$

where, i and j indicate the longitude and latitude respectively and $\Delta S_{i,j}$ is the area of the assigned grid point. In the current analysis field, the disturbance wind is strong enough in the analyzed typhoon vortex region so the disturbance radius r_0 can be determined from the profile of $\bar{V}_D(r)$ that defined the circular mean of V_D at a radius (r) from the center (λ_0, φ_0). Empirically the $\bar{V}_D(r)$ decreases with radius after it attains a maximum and reaches a relatively small value level at which the radius r_0 can be specified. Alternatively, the r_0 would be set to a limit if above profile could not be met. Then the average along the periphery of h_D at the radius

r_0 can be calculated as follows :

$$\bar{h}_D(r_0) = \frac{1}{2\pi} \oint h_D(r_0, \theta)\, d\theta \qquad (30)$$

By Eqn. (25), an axisymmetric analyzed typhoon vortex will be finally isolated from the analysis field. Its intensity decreases smoothly from the center to zero at the filtering edge.

Then the h_E can be calculated from the Eqn. (21) and will be used for the environmental field where the bogus typhoon be set up.

5. Typhoon bogus

The empirical method is applied to use the available surface parameters, such as the observed typhoon positions at current time and previous 12 hours, central pressure, radius of 15 m/s winds etc., to construct a bogus typhoon and blend it with the large-scale environmental field as the composite initial condition for the model forecast.

Following the work by Iwasaki (1987), the revised typhoon bogus scheme is described briefly as below.

5.1. *Surface pressure field*

The Fujita formula (1952) is used to define a symmetric surface pressure distribution as follows :

$$p(r) = p_E - \Delta p \left[1 + (r/R_0)^2 \right]^{-1/2} \qquad (31)$$

where, p_E is the mean environmental pressure, Δp is the difference between p_E and the observed central pressure. R_0 is the factor to determine the profile of the radial pressure gradients around the typhoon vortex center. It is decided by the radius of 15 m/s winds (R_{15}) and the Eqn. (31). Here R_0 is limited to no less than 30 km.

5.2. *Upper anticyclone*

Above the cloud top level (p_t), it is assumed that an anticyclone exists and the D-value is used to describe the deviation between typhoon and environmental field. The D-value is defined as,

$$D(r, p_t) = \begin{cases} ar^2 + b & r > R_0 \\ cr + d & R_0 < r < R_1 \\ e(r - R_E)^2 & R_1 < r < R_E \end{cases} \qquad (32)$$

where, R_1 and R_E are proportional to R_{15}. The parameters b and Δp represent the strength of the upper anticyclone at p_t level at which the environmental temperature sounding is intersected with the wet adiabatic profile rising from the sea surface. The parameters a, c, d and e can be calculated by the conditions that keep D-value profile changing smoothly at the points R_1 and R_E. Let D-value and its first-order difference be equal at the two points, the following formula can be derived as follows :

$$\begin{cases} aR_0^2 + b = cR_0 + d \\ cR_1 + d = e(R_1 - R_E)^2 \\ 2aR_0 = c \\ c = 2e(R_1 - R_E) \end{cases} \qquad (33)$$

Using the given R_0, R_1, R_E and b values, the parameters a, c, d and e are computed using the above formula and the anticyclone will be determined with assumption that the D-value vanish at 20 hPa (p_{mid}), *i.e.*,

$$D(r, p_{mid}) = 0 \qquad (34)$$

5.3. *Typhoon warm core*

The vertical profile of the temperature at bogus typhoon center below the cloud top level (p_t) is prescribed by,

$$T(0, p) = C_1 [T_c(p) - T_E(p)] + T_E(p) \qquad (35)$$

where, T_E is the environmental temperature. T_c is the moist adiabatic temperature rising from sea surface temperature. The constant C_1 is determined by the D-value from the deviation between T_c and T_E at p_t level according to the static equilibrium and the Eqn. (32).

Above the cloud top level (p_t), assuming the temperature at typhoon center, vary with logarithmic pressure along parabola, it is given by

$$T(0, p) = C_2 (\ln p - \ln p_{mid})(\ln p - \ln p_t) + T_E(p) \qquad (36)$$

where, the constant C_2 is defined from Eqns. (31) and (33) and the static relationship. Then the D-value at typhoon center at the pressure layers can be determined from the temperature deviation between

T_c and T_E.

At other radii, the distributions of D-value are specified from the formula:

$$D(r, p) = \alpha(r)\, D(0, p) + \beta(r) \tag{37}$$

The coefficients α and β are determined by Eqns. (31) and (32) below the cloud top level (p_t) and by Eqns. (32) and (34) above p_t then written as,

$$\alpha(r) = [D(r, p_s) - D(r, p_t)] \,/\, [D(0, p_s) - D(0, p_t)] \qquad (p \le p_t)$$

$$\beta(r) = [D(r, p_t)\, D(0, p_s) - D(0, p_t)\, D(r, p_s)] \,/\, [D(0, p_s) - D(0, p_t)]$$

and

$$\alpha(r) = \frac{D(r, p_t)}{D(0, p_t)} \quad (p \ge p_t)$$

$$\beta(r) = 0$$

where, p_s represents the sea surface level where the D-value is calculated from Eqn. (31) and the static relationship. Moreover, the moisture distribution is given by 90% relative humidity around the typhoon below the cloud top level (p_t).

5.4. *Gradient wind field*

The maintenance of typhoon circulation depends on the convergence at the lower layer. So the steady momentum equations neglecting the vertical advection are used to calculate the gradient wind. Including surface friction this equation in the cylindrical coordinate can be reduced as,

$$v_r \frac{\partial v_r}{\partial r} - \frac{v_\theta^2}{r} - f v_\theta + \frac{\partial \phi}{\partial r} + C_d \,|\, v \,|\, v_r = 0$$

$$v_r \frac{\partial v_\theta}{\partial r} + \frac{v_r\, v_\theta}{r} + f v_r + C_d \,|\, v \,|\, v_\theta = 0 \tag{38}$$

where, v_r and v_θ are radial wind and tangential wind component respectively, f is the Coriolis parameter, C_d represents the drag coefficient and ϕ is the geopotential height. In the upper troposphere, assumption is made that the divergence be set to compensate the convergence at the lower layers.

5.5. *Typhoon initial motion*

The initial movement vector is determined from the positions with a 12 hours interval. This vector is then uniformly added to the wind field of the bogus typhoon. The compensation for the mass field associated with the initial vector is neglected here.

5.6. *Implantation of bogus typhoon in the environment*

The bogus typhoon vortex is superposed on to the original analysis field using the weighted mean technique as follows,

$$f(r, \theta) = f_m\,(r, \theta)\, w(r) + f_E\,(r, \theta)\,[1 - w(r)] \tag{39}$$

where, f_m and f_E are bogus typhoon and analysis field respectively, the radius and azimuth angle (r, θ) denote the grid points in polar coordinate. The weight coefficient $w(r)$ is defined as,

$$w(r) = \begin{cases} 1 & r \le R_{inner} \\ \cos\left(\dfrac{\pi}{2} \cdot \dfrac{r - R_{inner}}{R_{outer} - R_{inner}}\right) & R_{inner} \le r \le R_{outer} \\ 0 & R_{outer} \le r \end{cases} \tag{40}$$

where R_{inner} and R_{outer} are proportional to R_{15}.

6. Operational results

The first version of MTTP had been completed with the simple physical processes and a lower horizontal resolution (approximately 100 km) by the end of 1992. In the next year, 26 forecasts were made for 10 typhoons or TCs locating in the model domain, which the prediction capabilities of MTTP were initially tested and the results showed feasible. In 1994, total 89 real-time forecasts for 23 typhoons or TCs were produced by MTTP for its further experiments and some of them were used as reference in operation. The results showed that the model was encouragingly skillful in forecasting typhoon tracks but poor in maintaining their central pressures and had somewhat trouble in the false spin-up in the initial time (not presented here). The problem, most possibly, was mainly due to the lower horizontal resolution, the simpler physics package and the incomplete initialization scheme.

Based on the above experiments, the main improvements were made for the MTTP in 1995 including the introduction of complex physics package instead of the simple one, a higher horizontal resolution

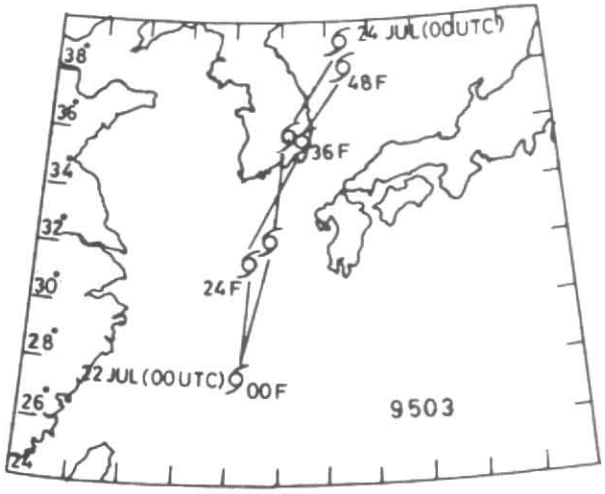

Fig. 1. The observed and predicted tracks of typhoon Faye (T9503)

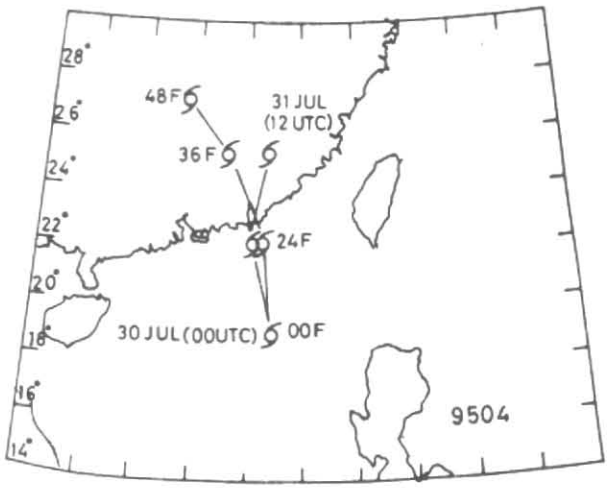

Fig. 2. The observed and predicted tracks of severe tropical storm Gray (T9504)

TABLE 1

Average track errors of MTTP forecasts (km)*

Year	t = 24 hours	t = 48 hours
1993	167 (26)	382 (23)
1994	196 (89)	361 (61)
1995	183 (85)	332 (69)

*The numbers in parentheses denote the forecast cases

(about 50 km) upgraded from the coarser one (about 100 km) and a new typhoon initialization scheme. The revised version of MTTP was installed and upgraded in quasi-operation from 1 June 1995. Then MTTP run for 85 forecasts of 17 typhoons or TCs and its products were used in the real-time operation for typhoon track prediction by NMC (Beijing). Its forecast track error statistic and those during the prior two years are presented as Table 1.

Some forecast cases of the typical typhoons or TCs that affected the coast of China are presented in detail below and shown in Figs. 1-6, where the character Fs denote the forecast central positions of typhoon or TC while the character Zs are the corresponding observed ones.

6.1. *The events of recurvature: typhoon Faye (T9503), tropical severe storm Gary (T9504) and tropical severe storm Helen (T9505)*

T9503 was a case of northward recurvature typhoon that made landfall on the South Korean coast on the mid-night of 23 July 1995. Total six day forecasts for the case were made from 18 July and the MTTP simulated the typhoon's northward tendency realistically. Among them, the forecasts on the two days of 18 and 20 July were better than those on 19 and 21 July. The best one is the forecast on 22 July prior to the date of landfall, which the model succeeded in predicting the landfall location and the landfall time (Fig. 1).

T9504 is also a recurvature case and the TC finally landed on the area between Chenghai and Yaopin in Guangdong Province of China. The TC moved west since it formed on 0600 UTC 29 July 1995. Generally it was estimated that it would keep its motion westward, but in fact it turned north rapidly from the mid-night of 30 July due to the influence by the development of South-Sea anticyclone. This recurvature process was simulated successfully by the model based on the data of 0000 UTC 30 July (Fig. 2). The encouraging forecasts for T9503 and T9504 brought the MTTP to the attention of the forecasters at NMC (Beijing).

The case T9505 is similar to T9504. Formed on 1200 UTC 9 August 1995, the TC shifted westward then rapidly turned north and made landfall on the area between Shenzhen and Huiyang in Guangdong Province of China. A series of forecasts for the TC were made with model running twice a day. The model was successful in forecasting the TC movement tendency, among which the second and the fourth were better than the first and the third. The forecast

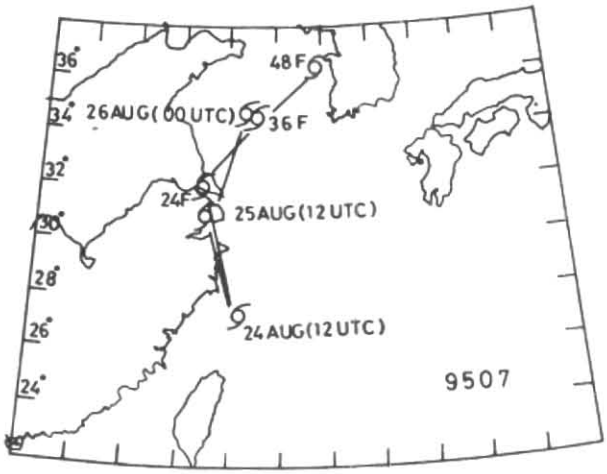

Fig. 3. The observed and predicted tracks of severe tropical storm Helen (T9505)

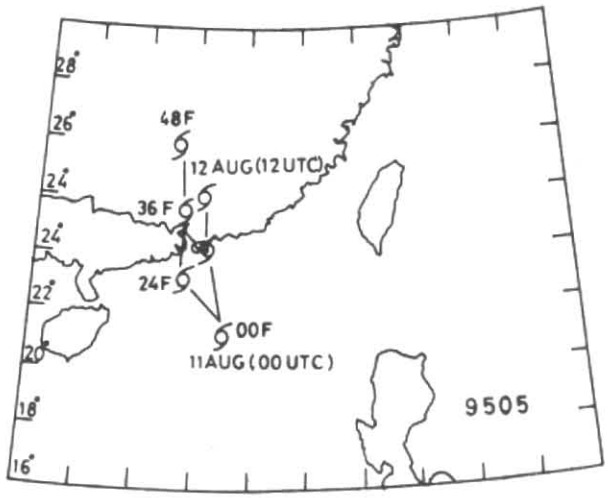

Fig. 4. The observed and predicted tracks of severe tropical storm Janis (T9507)

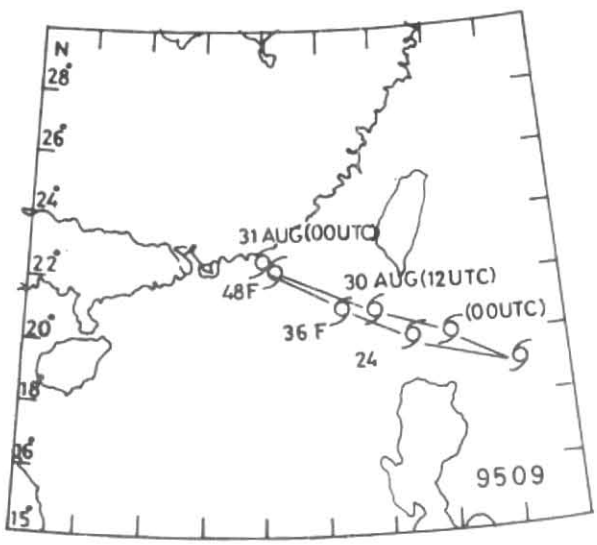

Fig. 5. The observed and predicted tracks of severe tropical storm Lois (T9508)

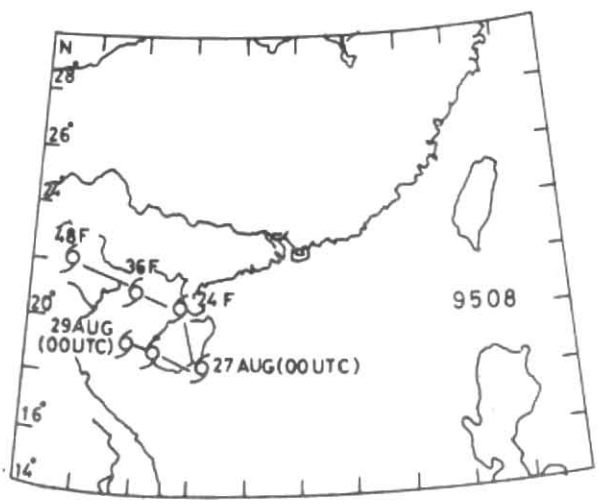

Fig. 6. The observed and predicted tracks of typhoon Kent (T9509)

TC position errors for landfall compared with the observation were considerably little (Fig. 3).

6.2. *The case with re-entry to sea: tropical severe storm Janis (T9507)*

The TC moved northwest after it formed and landed on Shitang town of Wenlin in Zhejiang Province of China in the morning of 25 August 1995. Then it turned northeast and entered Yellow-Sea again to shift to the Korean. The forecasts of MTTP were made from 1200 UTC 22 August and the model simulated the TC movement tendency realistically. Compared with the 48-hour forecasts, the 24-hour ones were better for the TC recurvature and its landfall time and location (Fig. 4).

6.3. *The event affected by the island orography: tropical severe storm Lois (T9508)*

This TC formed on the South-Sea and then made landfall rapidly on Wangning in Hainan Province of China in the morning of 28 August 1995. The MTTP had a little bad performance in landfall of this case (Fig. 5). Initial diagnosis and other prior studies showed that the effect of island orography on typhoons or TCs had not been expressed well in the current model design (not presented here).

6.4. *The case of rapid acceleration: typhoon Kent (T9509)*

This typhoon did not recurve but moved slowly on the sea surface on the east of Philippine. From 29 August 1995, it accelerated rapidly and then landed on the coast between Haifong and Huidong in Guangdong Province of China in the afternoon of 31 August. The model had large forecast error in simulating the typhoon's slow shift but had excellent performance in its rapid motion from 29 August. Especially the prediction for landfall location and time was very realistic (Fig. 6).

7. Conclusions

From above MTTP forecast cases and the performance of this model in both 1994 and 1995, it could be indicated that the MTTP had the considerable capability in the prediction of typhoons or TCs whose tracks were normal, and somewhat skills for other abnormal tracks such as those turning or accelerating rapidly. These results showed that the MTTP had a position in the real-time operation with its useful forecast production. However, the MTTP still had inability in some aspects and its improvement will be continued in the coming future.

Acknowledgements

The authors are grateful to Drs. Yulin Zhang and Xiaoren Guo, who mainly constructed the original and the current operational LAFS model respectively, for making available the LAFS model. Thanks are extended to the staff Mss. Xujun Ma, Fong Wan, Diangxia Zhang, Fang Zhao and Li Chao and Mr. Deyong Xu who participated in the work for current operational MTTP.

References

Anthes, R.A., 1977, "A cumulus parameterization scheme utilizing a one dimensional model", *Mon. Wea. Rev.*, **105**, 270-286.

Charnock, H., 1995, *Quant. J. Roy. Meteor. Soc.*, **81**, 639-640.

DeMaria, M., 1985, "Tropical cyclone motion in a non-divergent barotropical model", *Mon. Wea. Rev.*, **117**, 721-727.

Fels, S.B. and Schwarzko, M.D., 1975, "The simplified exchange approximation: a new method for radiative transfer calculations", *J. Atmos. Sci.*, **32**, 1475-1488.

Guo, X.R., Yang, Z.H. *et al.*, 1992, **Part 3**: "The limited area analysis and forecast (model) system", *The numerical Medium-range weather forecast and the application of its products.* National Meteorological Center (ed., in Chinese), China, 286-302.

Hart, T.L., Bourke, W., McAvaney, B.J., Forgan, B.W. and McGregor, J.L., 1988, "Atmospheric general circulation simulation with the BMRC global spectral model: The impact of revised physical parameterizations", *BMRC Research Report* No. 12, Bur. Met. Australia, 77pp.

Holland, G.J., 1984, "Tropical cyclone motion: A comparison of theory and observations", *J. Atmos. Sci.*, **41**, 68-75.

Iwasaki, T., Nakano, H. and Sugi, M., 1987, "The performance of a typhoon track prediction model", *J. Meteor. Soc., Japan*, **65**, 555-570.

Kuo, H.L., 1974, "Further studies of the parameterization of the influence of cumulus convection on large-scale flow", *J. Atmos. Sci.*, **31**, 1232-1240.

Kurihara, Y., Bender, M.A., Tuleya, R.E. and Ross, R.J., 1990, "Prediction experiments of hurricane Gloria (1985) using a multiply nested movable mesh model", *Mon. Wea. Rev.*, **118**, 2185-2198.

Kurihara, Y., Bender, M.A. and Ross, R.J., 1993, "An initialization scheme of hurricane models by vortex specification", *Mon. Wea. Rev.*, **121**, 2030-2045.

Lacis, A.A. and Hansen, J.E., 1974, "A parameterization for the absorption of solar radiation in the earth's atmosphere", *J. Atmos. Sci.*, **31**, 118-133.

Louis, J.F., 1979, "A parametric model of vertical eddy forces in the atmosphere", *Bound. Lay. Met.*, **17**, 187-202.

Puri, K., Davidson, N.E., Leslie, L.M. and Logan, L.W., 1992, "The BMRC tropical limited area model", *Aus. Meteor. Mag.*, **40**, 81- 104.

Tibaldi, S., 1982, "The production of a high resolution global orography and associated climatological surface fields for operational use at ECMWF", *Rivista Di Meteorologia Aeronautica* **V. XLII**, 285-308.

Tiedtke, M., 1984, "The sensitivity of time mean large-scale flow to cumulus convection in the ECMWF model", *Report of Workshop on Convection in the ECMWF model*, 28 November-1 December 1983, Shinfield Park, Reading, UK.

Tiedtke, M., 1987, "Parameterization of cumulus convection in large-scale numerical models", *The Physical Basis of Climate Modeling*, M.E. Schlesinger (ed.), NATO ASI Series, D. Reidel Publ. Co.

Wang, S.W. and Li, J.J., 1994, "Experiments of the real-time numerical weather prediction of typhoon tracks", *Quart. J. Applied Meteor.*, China (in Chinese), **5**(4), 462-469.